Bilanin-Artigado, C.; Tiburcio, E.; Ferrando-Soria, J.; Armentano, D.; Leyva Perez, A.; Pardo, E. (2021). Crystallographic Visualization of a Double Water Molecule Addition on a Pt-1-MOF during the Low-temperature Water-Gas Shift Reaction. ChemCatChem. 13(4):1195-1200. https://doi.org/10.1002/cctc.202001492

Crystallographic Visualization of a Double Water Molecule Addition on a Pt_1-MOF during the Low-temperature Water-Gas Shift Reaction

Cristina Bilanin,[a] Estefanía Tiburcio,[b] Jesús Ferrando–Soria,[a] Donatella Armentano*[c] Antonio Leyva–Pérez,*[a] and Emilio Pardo*[b]

[a] Cristina Bilanin, Dr. A. Leyva–Pérez.
Instituto de Tecnología Química
Universidad Politècnica de València–Consejo Superior de Investigaciones Científicas.
Avda. de los Naranjos s/n, 46022, València, Spain
E–mail: anleyva@itq.upv.es.

[b] E. Tiburcio, Dr. J. Ferrando–Soria, Dr. E. Pardo
Instituto de Ciencia Molecular (ICMol)
Universidad de Valencia
46980 Paterna, València, Spain
E-mail: emilio.pardo@uv.es

[c] Dr. D. Armentano.
Dipartimento di Chimica e Tecnologie Chimiche
Università della Calabria
87030 Rende, Cosenza, Italy.
E–mail: donatella.armentano@unical.it

Supporting information for this article is given via a link at the end of the document.

Abstract: The low-temperature water-gas shift reaction (WGSR, CO + H_2O ⇔ H_2 + CO_2) is considered a very promising reaction –candidate for fuel cells– despite an efficient and robust catalyst is still desirable. One of the more prominent catalysts for this reaction is based on single Pt atoms (Pt_1) on different supports, which are supposed to manifold the reaction by the accepted mechanism for the general WGSR, i.e. by addition of one H_2O molecule to CO, with generation of CO_2 and H_2. Here we show, experimentally, that not one but two H_2O molecules are added to CO on the Pt_1 catalyst, as assessed by a combination of reactivity experiments with soluble Pt catalysts, kinetic and spectroscopic measurements, and finally by *in-operando* single crystal X-ray diffraction on a Pt_1-MOF, to visualize the formation of the ~~formaldehyde~~ hemiacetal intermediate on the solid catalytic site. These results confirm our previous DFT predictions and provide a paradigmatic shift in the assumed mechanism of the WGSR, which may open the debate if two H_2O molecules are recurrently added during the WGSR, not only for Pt_1 catalysts but also for other metal catalysts.

Introduction

The development of novel more efficient and less costly methods for hydrogen production is a highly desired objective due to its multiple potential industrial uses[1] which, in addition, can play a pivotal role in the decarbonization of today's economy. In particular, the water-gas shift reaction[1,2] (WGSR, CO + H_2O ⇔ H_2 + CO_2) has not only emerged –in combination with coal gasification– as an important source of pure hydrogen[3] but, in addition, for the removal of carbon monoxide, which can be particularly important in hydrocarbon reforming processes where H_2 is usually contaminated with CO.[4] In fact, WGSR participates in industrial processes such as the Fischer–Tropsch process[5] (balancing the H_2/CO ratio) and the synthesis of methanol or ammonia.[6] Besides, the low-temperature WGSR is the preferred reaction in fuel cells,[7] where the temperature should not exceed ideally of 200 ºC. Despite these remarkable applications and related advances in the last years,[4,8–15] the search for optimal catalysts, with easy implementation in industry, still continues.

At present, there is still great controversy regarding the mechanism(s) operating in the low-temperature WGSR, which seems to depend strongly on reaction conditions (temperature being foremost among such conditions) as well as the chosen catalyst, usually metal oxides or a solid supported metal species.[16] So far, two possible mechanisms for the WGSR have been proposed: An associative mechanism and a "redox" regenerative one which is probably operative only at high temperatures.[4] In any case, none of these mechanisms assume a double addition of H_2O on CO, neither experimental or theoretically.[17] A total understanding of the mechanism would undoubtedly contribute to the design of more efficient active species capable to outperform industrially used catalysts.

In this context, we recently reported[18] the postsynthetic[19–24] preparation and structural characterization of well–defined Pt_1^{1+} single atom catalysts (SACs) supported, stabilized and homogeneously distributed within the pores of a robust metal-organic framework[25–30] (MOF). This hybrid material, with formula $[Pt^{2+}_2(\mu\text{–}O)(OH)_2(NH_3)_4]_{0.5}Pt^{1+}_1@Na_3\{Ni^{2+}_4[Cu^{2+}_2(Me_3mpba)_2]_3\} \cdot 79H_2O$ (**1**),[18] was characterized, in detail, by single crystal X-ray diffraction[31,32] and exhibited good catalytic activity for the WGSR at low–temperature. DFT calculations suggested an associative catalytic mechanism where both the coordinated Pt_1^{1+} metal and the hydrogen-bonded water molecules cause a double water attack mechanism to CO giving CO_2 with both oxygen atoms coming from water.

In this contribution, we have explored the catalytic activity of a variety of soluble mononuclear Pt compounds, for the sake of comparison with Pt_1^{1+} SACs and aiming at further confirming the proposed associative mechanism at low temperatures. In addition, *in-situ* single crystal X-ray diffraction (SCXRD) using synchrotron radiation on single crystals of MOF **1** in the presence of CO(g) and H_2O (g), has allowed us to unveil the crystal structure of a new host-guest adsorbate $[Pt^{1+}_2(\mu\text{-}O)(CO)_2(H_2O)_4]_{0.5} \cdot (CO_2)_2@Na_4\{Ni^{2+}_4[Cu^{2+}_2(Me_3mpba)_2]_3\} \cdot 16H_2O$ (**CO@1**) that permits the direct observation of the coordination

site for CO as well as the direct attack of two H_2O molecules to give the corresponding hemiacetal intermediate, ready to collapse into CO_2 and H_2. One of the H_2O molecules comes from the MOFs´ walls, in accordance with recent findings on the key role of adsorbed OH species in the reverse WGSR.[33] The robustness of the MOF **1** crystal is paramount to visualize H_2O molecules under reaction conditions, a typically difficult task.[34] These findings, in combination with isotopic and NMR experiments, strongly suggest that the double H_2O attack is general for any Pt_1 catalyst, soluble or supported, during the low-temperature WGSR.

Results and Discussion

Catalysis

The WGSR has been studied for more than fifty years as an undesired reaction of soluble Pt(0) complexes, since $Pt(CO)_n$ complexes tend to decompose in the presence of water under certain conditions.[35,36] However, it is difficult to find in the literature specific studies regarding soluble cationic Pt complexes as catalysts for the WGSR, perhaps because the most stable and available Pt chloride compounds such as cisplatin $PtCl_2(NH_3)_2$ and K_2PtCl_4 early showed no catalytic activity.[37,38] Figure 1 shows the structure of the cationic Pt complexes **2-5** used here as catalysts for the WGSR. Cisplatin **2** and complex **3**[39] are typical Pt(II) chloride complexes with significantly different solubility in water, the aqueous complex **4**[40] is representative of a potential WGSR intermediate with H_2O, and complex **5**[41] is also representative of a potential WGSR intermediates with CO. In particular, stoichiometric amounts of complex **5** have shown to give the WGSR in the presence of water, with the uncoordinated pyrazolyl ligand acting as an anchoring site for the reacting H_2O molecules, just the role of the walls in MOF **1**.[41] However, no catalytic uses in the WGSR have been reported to date, as far as we know.

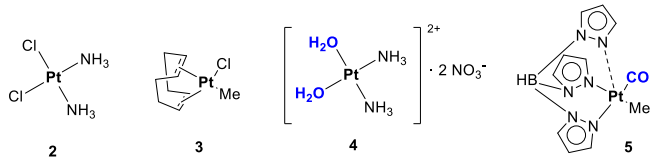

Figure 1. Pt complexes used as catalysts in this work for the low-temperature water-gas shift reaction (WGSR). In bold, the Pt atom; in blue, ligands that act as reactants during the WGSR.

Table 1 shows the catalytic results for the low-temperature WGSR with MOF **1**, with a reported and very active Pt_1-Na/SiO_2 solid catalyst,[8,10] and with complexes **2-5**, H_2PtCl_4 and commercially available Pt NPs on charcoal (10 wt%). It can be seen that MOF **1** is much more active than any other Pt catalyst tested (entry 1), with an initial turnover frequency (TOF_0) = 40 h^{-1} under the indicated reaction conditions. As expected, Pt chloride compounds, including complexes **2** and **3**, and Pt-C were completely inactive (entries 2-5), however, complexes **4-5** were reasonably active for the reaction, approaching the catalytic activity of the state-of-the-art solid catalyst Pt_1-Na/SiO_2 (entries 6-9, see also Figures S1-S3 in the Supporting Information).

Table 1. Catalytic results for the low-temperature WGSR with different Pt catalysts. Reaction conditions: 1 mmol CO, 5.5 mmol H_2O, 0.001 mmol (0.1 mol%) of Pt, 140 ºC, total pressure= 5 bar (2.5 bar of N_2).

Run	Catalyst	P(CO) (bar)	H_2O (μL)	TOF_0 (h^{-1})[a]
1	MOF **1**	2.5	100	40.0
2	H_2Cl_6Pt	2.5	100	N.D.
3	Pt-C	2.5	100	N.D.
4	$PtCl_2(NH_3)_2$ **2**	2.5	100	N.D.
5	PtClMe(COD) **3**	2.5	100	N.D.
6	$[Pt(NH_3)_2(H_2O)_2](NO_3)_2$ **4**	2.5	100	1.24
7		2.5	0	2.89
8	Pt(Me)[HB(pz)$_3$]CO **5**	0	100	0.53
9	Pt_1-Na/SiO_2	2.5	100	7.2

[a] Measured as mmol of CO_2 generated by mmol of Pt during the linear initial rate: N.D.: non-detected. Results are an average of two different batches.

Complexes **4** and **5** can be used as both catalyst and reagent for the WGSR, to give TOF_0s= 2.89 and 0.55 h^{-1}, respectively (entries 6-8). These results indicate that the activation of CO in the pre-formed aquo Pt complex is feasible, and also the opposite, the activation of H_2O in the carbonyl Pt complex, although less efficiently. These results are in good agreement with the previously proposed mechanism for MOF **1**,[18] where CO coordinates and activates onto the hydrated Pt_1 site.

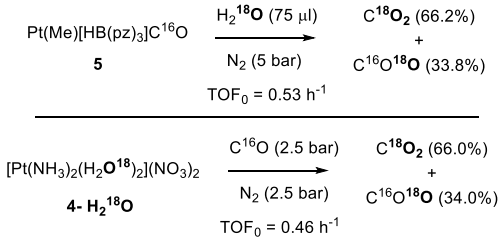

Figure 2. Isotopically labelled experiments with stoichiometric amounts of Pt complexes containing one of the reactants for the low-temperature water-gas shift reaction (WGSR).

Figure 2 shows the result for the reaction between the carbonyl complex **5** and $H_2{}^{18}O$, in the absence of any other water molecule or CO atmosphere. This experiment is designed to assess if one or two H_2O molecules are coupled to CO on the soluble Pt complex, to give CO_2 with both oxygen atoms coming from water. The results show that $C^{18}O_2$ is formed twice than $C^{16}O^{18}O$, the statistial result for a double addition of $H_2{}^{18}O$ (Figure S4). Since the high excess of $H_2{}^{18}O$ may give the isotopically marked product after extensive equilibria, a new experiment was carried out with the isotopically labelled aquo complex $[Pt(NH_3)_2(H_2O^{18})_2](NO_3)_2$ (**4-$H_2{}^{18}O$**), and the reaction of **4-$H_2{}^{18}O$** with CO gives, as shown in Figure 2, the same $C^{18}O_2$ distribution (64.0%) and a similar TOF_o (0.46 h^{-1}) than in excess of water (Figure S5). The similar CO_2 distribution indicates a double H_2O addition on CO with the cationic Pt complexes, and the similar initial rate strongly supports that both CO and H_2O participate in the rate-determining step of the reaction, as occurs with MOF **1**.[18]

Figure 3 shows the ^{13}C magic angle spinning solid-state nuclear magnetic resonance (MAS NMR) of MOF **1** when isotopically labelled ^{13}CO was co-adsorbed with water (^{13}CO:H_2O 1:2 equivalents respect to Pt) into a sealed rotor and heated.[18] It can be seen the appearance a new signal at 156 ppm, which transforms into $^{13}CO_2$ after heating. The shift of this signal fits well with the hemiacetal orthoformate $H^{13}C(OH)_3$ (predicted 140 ppm), and cross polarization (CP) NMR experiments confirm that the ^{13}C atom bears H atoms at 1–2 bond distance. This result explains the statistical $C^{18}O_2$ distribution found for MOF **1**[18] and also above for Pt complexes **4** and **5**, since the hemiacetal intermediate collapses into CO_2 and H_2O (and also H_2) with the same probability for the 3 oxygen atoms.

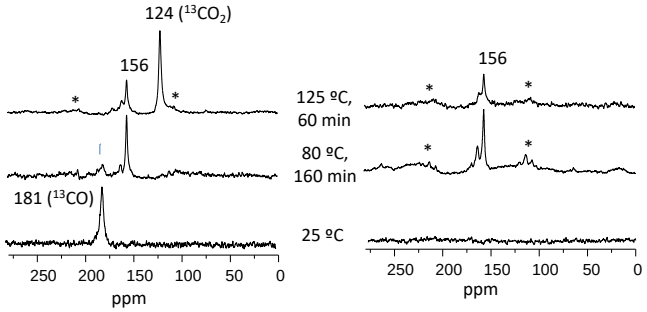

Figure 3. ^{13}C MAS NMR (left) and the corresponding CP–NMR (right) of ^{13}CO on MOF **1**, co–adsorbed with water (1:2:1 in Pt) and heated at the indicated temperature and time. * Indicates spinning side bands.

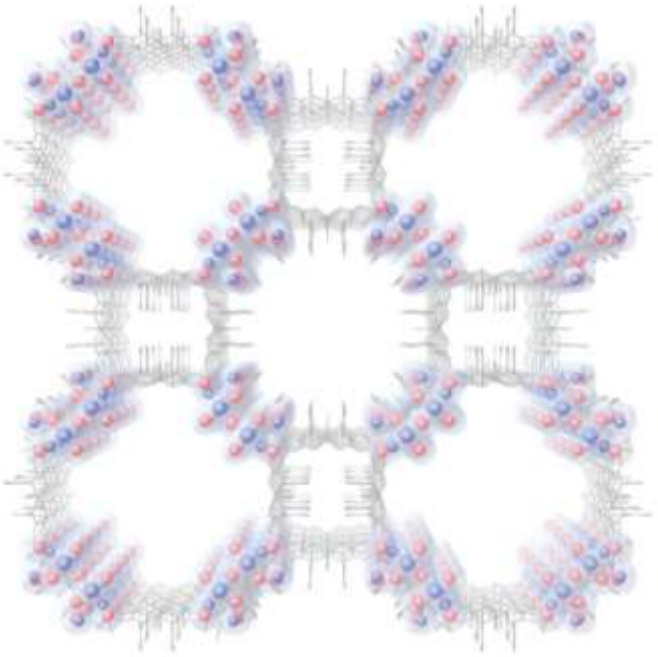

Figure 4. Crystal structures, determined by synchrotron X-ray diffraction, of the **CO@1** obtained from the *in-situ* simulation of WGSR: Perspective view along *c* crystallographic axis, showing $[Pt^{1+}{}_2(\mu\text{-}O)(CO)_2(H_2O)_4]$ moieties and CO_2 molecules embedded in pores. The heterobimetallic CuNi 3D anionic network is depicted as grey sticks. Pt(I) cations in the pores and carbon atoms of CO molecules are represented by blue spheres whereas oxygen atoms are depicted in red. Surface with Van der Waals radii is used to highlight the generated molecules within MOFs channels. Sodium cation and crystallization water molecules in the pores have been omitted for clarity.

Crystal Structure of CO@1

In-situ SC-XRD experiments were carried out for MOF **1** at a temperature of 310 K and under the presence of CO/H_2O mixture, using synchrotron radiation, on single crystal sealed in the gas cell, designed and built at Diamond Light Source, in the I19 beamline (Figure S6).

The sample was sealed in that specially designed cell and the the CO/Ar gas mixture through a heated water bubblier (to generate the CO/H_2O mixture) was fluxed under a pressure of 1.12 bar for 15 min. The crystal structure of **CO@1** was determined at 310 K. It results isoreticular to **1**, crystallizing in the *P*4/*mmm* space group of the tetragonal system (Table S1), with the anionic $Ni^{II}{}_4Cu^{II}{}_6$ open–framework structure accommodating Pt-CO adducts and free CO_2 molecules (Figures 4-5, S7-S10) in its hydrophilic and hydrophobic octagonal pores, respectively.

Detailed analysis of SCXRD data indicated that square planar Pt^{1+} atoms had been attached by one CO and two H_2O molecules. Furthermore, the highly hydrophilic environment stabilized an oxo bridge between two approaching complexes giving rise to dimers of formula $[Pt^{1+}{}_2(\mu\text{-}O)(CO)_2(H_2O)_4]$ (Figure 5a-b), thus confirming that it is the addition of both CO and two H_2O promoting the hemiacetal evolution into CO_2. Noteworthy, **CO@1** crystal structure unveils produced CO_2 molecules as well, within the MOF pores, residing in proximity of Pt intermediate. The crystal structure snapshotted the Pt-CO water adducts perfectly stabilized in hydrophilic pores (Figures 4-5 and S9), whereas CO_2 molecules reside in hydrophobic channels most likely as a direct consequence of the chemical stabilization provided by phenyl rings pointing within MOF pores (Figures 4 and S10-S11). Hydrogen bonds between H_2O surrounding Pt have a key role to guarantee those active interactions with acceptor oxygen atoms from the walls of the network [$CO\cdots O_{MOF}$ of 2.894 and $H_2O\cdots O_{MOF}$ of 3.156(4) Å]. On the contrary the *in-situ* generated CO_2 is stabilized by aromatic rings at a distance of 3.39 Å (Figure S11).

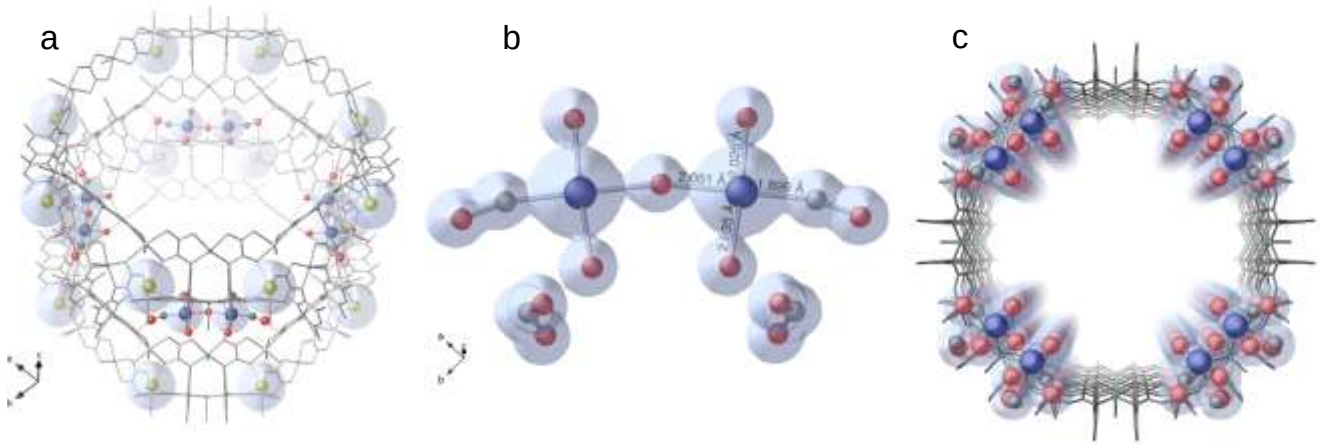

Figure 5. Perspective views showing details of **CO@1** crystal structure: a) Single pore side view of hydrogen bonds interactions stabilizing $[Pt^{1+}_2(\mu\text{-}O)(CO)_2(H_2O)_4]$ intermediates within hydrophilic pores; b) detailed crystal structure of $[Pt^{1+}_2(\mu\text{-}O)(CO)_2(H_2O)_4]$ moieties clarifying CO and H_2O binding sites; c) view down direction of pore's propagation showing (all in blue color) the in-situ generated molecules interacting with MOF's walls. Na^+ and Pt^+ in gold and blue ones, respectively. The heterobimetallic CuNi 3D anionic network is depicted as grey sticks. Carbon and oxygen atoms of the in-situ generated molecules, are depicted as grey and red spheres, respectively. Surface has been depicted to highlight Pt-CO water adducts and CO_2 hosted in pores.

The scope of this experiment design was to unequivocally visualize that two H_2O molecules are coupled to CO on the Pt complex, to give CO_2. Looking at the crystal structure of **CO@1** it is evident the geometric organization of the system in which CO molecule activates catalysts with a bind on *cis* arrangement respect to the two active H_2O molecules with optimal geometric requisites for nucleophilic attack. In the square planar Pt environment, the CO molecule is coordinated at a distance of 1.897(9) Å that result shorter than that of Pt-OH_2 bond lengths [2.035(9) and 2.026(9) Å].[18]

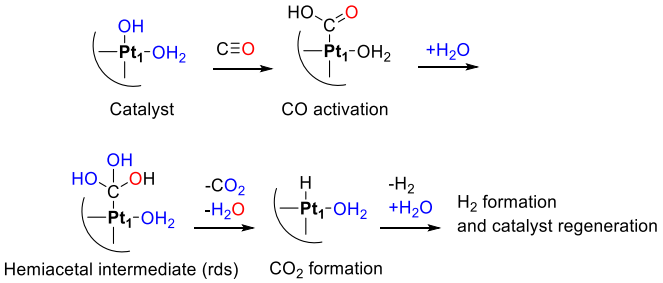

Figure 6. Proposed mechanism or the Pt_1-catalyzed low-temperature water-gas shift reaction (WGSR). The main product distribution is colored, although a statistical distribution indeed occurs.

With these results in hand, Figure 6 shows the proposed mechanism for the low-temperature WGSR with Pt_1 catalysts, either Pt complexes on single atom supported solids. First, CO activation occurs on the Pt_1 site, with the assistance of a coordinated hydroxyl group. Then, a second H_2O molecule coordinates and attacks the formyl intermediate, to give the corresponding hemiacetal. The formation of this intermediate on the catalytic site is the plausible rate-determining step (rds) of the reaction, not only on the basis of thermodinamic and kinetic parameters,[6b] but also suggested by its clear detection by MAS NMR. Then, the hemiacetal easily collapses into CO_2 in virtue of a favoured β-H elimination to give a gas molecule (CO_2) and to regenerate the catalyst after Pt hydride reaction, to give the second gas molecule, H_2. This mechanims showcases the key role of at least two H_2O molecules, adsorbed and coordinated, to trigger the low-temperature WGSR.

Conclusion

In summary, in this contribution we have tried to shed light on the mechanisms governing the low-temperature WGSR by using a multi-technique approach that includes catalysts, kinetic and spectroscopic measurements and, last but not least, *in-operando* single crystal X-ray diffraction on a Pt_1-MOF under the presence of a CO/H_2O mixture. SCXRD studies allow to visualize, for the first time, that square planar $Pt^{\delta+}$ SACs are simultaneously coordinated by one CO and two H_2O molecules –forming a Pt-CO water adduct perfectly stabilized in the hydrophilic pores of the MOF that suggests the formation of a ~~formaldehyde~~ hemiacetal intermediate– and also the resulting CO_2 molecules also hosted within the MOF channels. These results, together with the catalytic ones, validate the occurrence of an associative mechanism, with a double H_2O attack, for the low-temperature WGSR ~~for~~with any Pt_1 catalyst.

Experimental Section

Synthesis of Pt_1-MOF. MOF $[Pt^{2+}_2(\mu\text{-}O)(OH)_2(NH_3)_4]_{0.5}Pt^{1+}_1@Na_3\{Ni^{2+}_4[Cu^{2+}_2(Me_3mpba)_2]_3\} \cdot 79H_2O$ (**1**) was prepared and characterised as reported earlier.[18]

Synthesis of platinum complexes. The syntheses of PtClMe(COD) (**3**), $[Pt(NH_3)_2(OH_2)_2]^{2+}$ (**4**) and Pt(Me)[HB(pz)$_3$]CO (**5**) are thoroughly described in the Supporting Information.

General catalytic reaction procedure. The corresponding Pt catalyst (0.001 mmol) was placed in a 6.5 mL glass vial equipped with a valve and a manometer, and Milli-Q water (100 µL, 5.5 equiv.) was added. The vial was closed, purged three times with 5 bar of nitrogen and pressurized with

2.5 bar of CO (1 mmol) and 2.5 bar of nitrogen to a final pressure of 5 bar; the reaction mixture was heated to 140 ° C. Samples of the reaction mixture were drawn using a Hamilton SampleLock gas syringe and the reaction products were analyzed with an Agilent micro GC (Mosieve 5A column using argon as carrier gas). Experiments were repeated twice.

Reaction procedure with complex 5 and isotopically labelled $H_2{}^{18}O$. Complex **5** (1.7 mg, 0.73 mg de Pt) and 100 µL of labeled water ($H_2{}^{18}O$) were added to a 6.5 mL glass vial equipped with a valve and a manometer. The vial was closed, purged three times with 5 bar of nitrogen and pressurized with 5 bar of nitrogen (reagent CO is obtained from the catalyst); the reaction mixture was heated to 140 ° C. Samples of the reaction mixture were drawn and analyzed as above.

Reaction procedure with complex 4 or isotopically labelled complex 4-$H_2{}^{18}O$ as a reactant. Complex **4** or **4-$H_2{}^{18}O$** (1.2 mg, 0.6 mg of Pt) was placed in a 6.5 mL glass vial equipped with a valve and a manometer. The vial was closed (the water is obtained from the complex) and purged three times with 5 bar of nitrogen and pressurized with 2.5 bar of CO (1 mmol) and 2.5 bar of nitrogen to a final pressure of 5 bar; the reaction mixture was heated to 140 ° C. Samples of the reaction mixture were drawn and analyzed as above.

X-ray crystallographic details. The crystallographic studies on single-crystal X-ray on **1** were carried out at beamline I19 of Diamond Light Source. A crystal of **1** with 0.05 x 0.04 x 0.04 mm as dimensions was selected and mounted on a MITIGEN holder in glue, then the sample pin was inserted in the glass capillary, sealed in the cell and placed on the goniometer system under a controlled temperature at 310 K. The gas loading was precisely controlled and measured on single crystal sealed in the gas cell, to perform *in-situ* gas-dosing experiments. Without activation of the crystal (considering water is part of the gases mixture) data were acquired, measuring on **1** under the presence of the CO/H_2O mixture, under a pressure of 1.12 bar for 15 min. Once measurements were performed, the gas was exhausted from main rig and sample lines. Then, vacuum was applied on all the lines to remove any residue of previously measured toxic gas and all the rig and gas lines refilled with inert gas. Diffraction data for **1** were collected on using synchrotron radiation at I19 beamline of the Diamond Light Source at λ = 0.6889 Å. Crystal data: Tetragonal, space group *P4/mmm*, *T* = 310(2), *Z* = 4; $C_{81}H_{96}Cu_6N_{12}Na_4Ni_4O_{60}Pt$, *a* = 35.893(2) Å, *c* = 15.1253(10) Å, *V* = 19487(3) $Å^3$. Further details can be found in the Supplementary Information and Table S1. CCDC 2031954 contain the supplementary crystallographic data for **CO@1** reported in this paper. These data can be obtained free of charge *via* www.ccdc.cam.ac.uk/conts/retrieving.html or from the Cambridge Crystallographic Data Centre, 12 Union Road, Cambridge CB21EZ, UK; fax: (+44)1223-336-033; or deposit@ccdc.cam.ac.uk.

Acknowledgements

This work was supported by the Ministero dell'Istruzione, dell'Università e della Ricerca (Italy) and the MINECO (Spain) (Projects CTQ2016–75671–P and CTQ2017–86735–P and the excellence units "Severo Ochoa" SEV–2016–0683 and "Maria de Maeztu" CEX2019-000919-M). C. B. thanks ITQ for the concession of a fellowship. Thanks are extended to the "2019 Post–doctoral Junior Leader–Retaining Fellowship, la Caixa Foundation (ID100010434 and fellowship code LCF/BQ/PR19/11700011" (J. F.–S.). D.A. acknowledges the financial support of the Fondazione CARIPLO / "Economia Circolare: ricerca per un futuro sostenibile" 2019, Project code: 2019–2090, MOCA. We thank to Dr. R. Adam, Dr. J. Oliver-Meseguer and J. C. Arango for their help. E.P. acknowledges the financial support of the European Research Council under the European Union's Horizon 2020 research and innovation programme / ERC Grant Agreement No 814804, MOF–reactors

Conflict of Interest

The authors declare no conflict of interest.

Keywords: water gas shift • single atom catalyst • metal-organic framework • platinum • crystallography

[1] C. Ratnasamy, J. P. Wagner, *Catal. Rev.* **2009**, *51*, 325.
[2] D. S. Newsome, *Catal. Rev.* **1980**, *21*, 275.
[3] R. Burch, *Phys. Chem. Chem. Phys.* **2006**, *8*, 5483.
[4] S. Yao, X. Zhang, W. Zhou, R. Gao, W. Xu, Y. Ye, L. Lin, X. Wen, P. Liu, B. Chen, E. Crumlin, J. Guo, Z. Zuo, W. Li, J. Xie, L. Lu, C. J. Kiely, L. Gu, C. Shi, J. A. Rodriguez, D. Ma, *Science* **2017**, *357*, 389.
[5] D. B. Bukur, B. Todic, N. Elbashir, *Catal. Today* **2016**, *275*, 66.
[6] A. Ambrosi, S. E. Denmark, *Angew. Chemie Int. Ed.* **2016**, *55*, 12164.
[7] W. Vielstich, A. Lamm, H. A. Gasteiger, H. Yokokawa, Eds. , *Handbook of Fuel Cells*, John Wiley & Sons, Ltd, Chichester, UK, **2010**.
[8] Q. Fu, *Science* **2003**, *301*, 935.
[9] J. A. Rodriguez, S. Ma, P. Liu, J. Hrbek, J. Evans, M. Perez, *Science* **2007**, *318*, 1757.
[10] Y. Zhai, D. Pierre, R. Si, W. Deng, P. Ferrin, A. U. Nilekar, G. Peng, J. A. Herron, D. C. Bell, H. Saltsburg, M. Mavrikakis, M. Flytzani-Stephanopoulos, *Science* **2010**, *329*, 1633.
[11] M. Yang, S. Li, Y. Wang, J. A. Herron, Y. Xu, L. F. Allard, S. Lee, J. Huang, M. Mavrikakis, M. Flytzani-Stephanopoulos, *Science* **2014**, *346*, 1498.
[12] J. A. Rodriguez, P. J. Ramírez, G. G. Asara, F. Viñes, J. Evans, P. Liu, J. M. Ricart, F. Illas, *Angew. Chemie Int. Ed.* **2014**, *53*, 11270.
[13] P. J. Smith, S. A. Kondrat, P. A. Chater, B. R. Yeo, G. M. Shaw, L. Lu, J. K. Bartley, S. H. Taylor, M. S. Spencer, C. J. Kiely, G. J. Kelly, C. W. Park, G. J. Hutchings, *Chem. Sci.* **2017**, *8*, 2436.
[14] J. H. Carter, X. Liu, Q. He, S. Althahban, E. Nowicka, S. J. Freakley, L. Niu, D. J. Morgan, Y. Li, J. W. Niemantsverdriet, S. Golunski, C. J. Kiely, G. J. Hutchings, *Angew. Chem. Int. Ed.* **2017**, *56*, 16037.
[15] J. A. Rodriguez, J. Graciani, J. Evans, J. B. Park, F. Yang, D. Stacchiola, S. D. Senanayake, S. Ma, M. Pérez, P. Liu, J. F. Sanz, J. Hrbek, *Angew. Chemie Int. Ed.* **2009**, *48*, 8047.
[16] J. Resasco, L. DeRita, S. Dai, J. P. Chada, M. Xu, X. Yan, J. Finzel, S. Hanukovich, A. S. Hoffman, G. W. Graham, S. R. Bare, X. Pan, P. Christopher, *J. Am. Chem. Soc.* **2020**, *142*, 169.
[17] M. Torrent, M. Solà, G. Frenking, *Chem. Rev.* **2000**, *100*, 439.
[18] M. A. Rivero-Crespo, M. Mon, J. Ferrando-Soria, C. W. Lopes, M. Boronat, A. Leyva-Pérez, A. Corma, J. C. Hernández-Garrido, M. López-Haro, J. J. Calvino, E. V. Ramos-Fernandez, D. Armentano, E. Pardo, *Angew. Chemie Int. Ed.* **2018**, *57*, 17094.
[19] S. M. Cohen, *J. Am. Chem. Soc.* **2017**, *139*, 2855.
[20] M. Mon, J. Ferrando-Soria, M. Verdaguer, C. Train, C. Paillard, B. Dkhil, C. Versace, R. Bruno, D. Armentano, E. Pardo, *J. Am. Chem. Soc.* **2017**, *139*, 8098.

[21] F. R. Fortea-Pérez, M. Mon, J. Ferrando-Soria, M. Boronat, A. Leyva-Pérez, A. Corma, J. M. Herrera, D. Osadchii, J. Gascon, D. Armentano, E. Pardo, *Nat. Mater.* **2017**, *16*, 760.

[22] M. Tejeda-Serrano, M. Mon, B. Ross, F. Gonell, J. Ferrando-Soria, A. Corma, A. Leyva-Pérez, D. Armentano, E. Pardo, *J. Am. Chem. Soc.* **2018**, *140*, 8827.

[23] M. Mon, M. A. Rivero-Crespo, J. Ferrando-Soria, A. Vidal-Moya, M. Boronat, A. Leyva-Pérez, A. Corma, J. C. Hernández-Garrido, M. López-Haro, J. J. Calvino, G. Ragazzon, A. Credi, D. Armentano, E. Pardo, *Angew. Chemie Int. Ed.* **2018**, *57*, 6186.

[24] M. Mon, R. Bruno, J. Ferrando-Soria, L. Bartella, L. Di Donna, M. Talia, R. Lappano, M. Maggiolini, D. Armentano, E. Pardo, *Mater. Horizons* **2018**, *5*, 683.

[25] H. Furukawa, K. E. Cordova, M. O'Keeffe, O. M. Yaghi, *Science* **2013**, *341*, 974.

[26] M. Eddaoudi, D. F. Sava, J. F. Eubank, K. Adil, V. Guillerm, *Chem. Soc. Rev.* **2015**, *44*, 228.

[27] H.-C. "Joe" Zhou, S. Kitagawa, *Chem. Soc. Rev.* **2014**, *43*, 5415.

[28] A. Kirchon, L. Feng, H. F. Drake, E. A. Joseph, H.-C. Zhou, *Chem. Soc. Rev.* **2018**, *47*, 8611.

[29] G. Maurin, C. Serre, A. Cooper, G. Férey, *Chem. Soc. Rev.* **2017**, *46*, 3104.

[30] A. M. Rice, C. R. Martin, V. A. Galitskiy, A. A. Berseneva, G. A. Leith, N. B. Shustova, *Chem. Rev.* **2020**, *120*, 8790.

[31] M. Viciano-Chumillas, M. Mon, J. Ferrando-Soria, A. Corma, A. Leyva-Pérez, D. Armentano, E. Pardo, *Acc. Chem. Res.* **2020**, *53*, 520.

[32] R. J. Young, M. T. Huxley, E. Pardo, N. R. Champness, C. J. Sumby, C. J. Doonan, *Chem. Sci.* **2020**, *11*, 4031.

[33] M. Zhu, P. Tian, M. E. Ford, J. Chen, J. Xu, Y.-F. Han, I. E. Wachs, *ACS Catal.* **2020**, *10*, 7857.

[34] W. Yuan, B. Zhu, X.-Y. Li, T. W. Hansen, Y. Ou, K. Fang, H. Yang, Z. Zhang, J. B. Wagner, Y. Gao, Y. Wang, *Science* **2020**, *367*, 428.

[35] H. C. Clark, V. K. Jain, *Coord. Chem. Rev.* **1984**, *55*, 151.

[36] T. Yoshida, Y. Ueda, S. Otsuka, *J. Am. Chem. Soc.* **1978**, *100*, 3941.

[37] C.-H. Cheng, R. Eisenberg, *J. Am. Chem. Soc.* **1978**, *100*, 5968.

[38] C.-H. Cheng, L. Kuritzkes, R. Eisenberg, *J. Organomet. Chem.* **1980**, *190*, C21.

[39] M. Enders, B. Görling, A. B. Braun, J. E. Seltenreich, L. F. Reichenbach, K. Rissanen, M. Nieger, B. Luy, U. Schepers, S. Bräse, *Organometallics* **2014**, *33*, 4027.

[40] B. Surnar, K. Sharma, M. Jayakannan, *Nanoscale* **2015**, *7*, 17964.

[41] H. C. Lo, M. A. Iron, J. M. L. Martin, E. Keinan, *Chem. - A Eur. J.* **2007**, *13*, 2812.

Entry for the Table of Contents

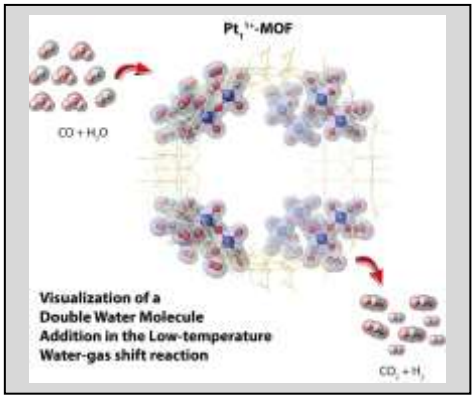

Herein, we show evidence that a double water attack occurs in the Pt-catalyzed low-temperature water-gas shift reaction (WGSR) by a combination of reactivity experiments with soluble Pt catalysts, kinetic and spectroscopic measurements and *in-operando* single crystal X-ray diffraction on a Pt_1-MOF. It allows a clear step forward on the understanding of the mechanism of the WGSR.